RESEARCH ARTICLE

Global Change Biology WILEY

Tree crown damage and its effects on forest carbon cycling in a tropical forest

Jessica F. Needham[1] | Gabriel Arellano[2,3] | Stuart J. Davies[4] | Rosie A. Fisher[5] | Valerie Hammer[6] | Ryan G. Knox[1] | David Mitre[7] | Helene C. Muller-Landau[7] | Daniel Zuleta[4] | Charlie D. Koven[1]

[1]Earth and Environmental Sciences Area, Lawrence Berkeley National Laboratory, Berkeley, California, USA

[2]Department of Ecology and Evolutionary Biology, University of Michigan, Ann Arbor, Michigan, USA

[3]Oikobit LLC, Albuquerque, New Mexico, USA

[4]Forest Global Earth Observatory, Smithsonian Tropical Research Institute, Washington, District of Columbia, USA

[5]CICERO Center for International Climate Research, Oslo, Norway

[6]University of California, Berkeley, Berkeley, California, USA

[7]Smithsonian Tropical Research Institute, Apartado, Repúblico de Panamá

Correspondence
Jessica F. Needham, Earth and Environmental Sciences Area, Lawrence Berkeley National Laboratory, Berkeley, CA, USA.
Email: jfneedham@lbl.gov

Abstract

Crown damage can account for over 23% of canopy biomass turnover in tropical forests and is a strong predictor of tree mortality; yet, it is not typically represented in vegetation models. We incorporate crown damage into the Functionally Assembled Terrestrial Ecosystem Simulator (FATES), to evaluate how lags between damage and tree recovery or death alter demographic rates and patterns of carbon turnover. We represent crown damage as a reduction in a tree's crown area and leaf and branch biomass, and allow associated variation in the ratio of aboveground to belowground plant tissue. We compare simulations with crown damage to simulations with equivalent instant increases in mortality and benchmark results against data from Barro Colorado Island (BCI), Panama. In FATES, crown damage causes decreases in growth rates that match observations from BCI. Crown damage leads to increases in carbon starvation mortality in FATES, but only in configurations with high root respiration and decreases in carbon storage following damage. Crown damage also alters competitive dynamics, as plant functional types that can recover from crown damage outcompete those that cannot. This is a first exploration of the trade-off between the additional complexity of the novel crown damage module and improved predictive capabilities. At BCI, a tropical forest that does not experience high levels of disturbance, both the crown damage simulations and simulations with equivalent increases in mortality does a reasonable job of capturing observations. The crown damage module provides functionality for exploring dynamics in forests with more extreme disturbances such as cyclones and for capturing the synergistic effects of disturbances that overlap in space and time.

KEYWORDS
aboveground biomass, canopy turnover, carbon residence time, crown damage, forest disturbance, mortality, tropical forests

1 | INTRODUCTION

Changes to the residence time of carbon in living vegetation are a major source of uncertainty in predictions of forest dynamics (Friend et al., 2014). Vegetation carbon residence time is largely defined by

tree mortality, which is thought to be increasing across large parts of the globe driven by rising temperatures and increases in disturbances such as wildfires, droughts and land use change (Carnicer et al., 2011; McDowell et al., 2018; Peñuelas et al., 2017; Senf et al., 2018).

Crown damage is an important predictor of individual tree mortality (Arellano et al., 2019; Reis et al., 2022). After light limitation, crown loss was found to have the largest impact on forest wide mortality out of 19 risk factors assessed across six tropical forests (Zuleta et al., 2021). A number of mechanisms could drive the damage-mortality relationship. Crown loss reduces photosynthesis, placing trees at increased risk of carbon starvation (McDowell et al., 2008). Damage to xylem vessels increases the risk of embolism and hydraulic failure (Adams et al., 2017). Wounds from branch loss provide entry points for pathogens and insects, which may lead to death from disease (Anderegg et al., 2015; Gaylord et al., 2013; Jönsson et al., 2012). Damaged trees may also be weakened structurally, making them vulnerable to wind throw (Csilléry et al., 2017).

Aside from the impact on mortality, crown damage itself accounts for a significant portion of total canopy turnover. In the 50-ha plot on Barro Colorado Island (BCI), Panama, a drone-based study of canopy disturbances found that branchfall accounted for 23% of the total area disturbed (Araujo et al., 2021). A ground-based study estimated that branchfall accounted for 17% of the total volume of woody debris (Gora et al., 2019). Analyses of tree census data estimated woody aboveground carbon fluxes from tree damage as 0.1–0.6 $Mg\,ha^{-1}\,year^{-1}$ of AGB loss, compared with 5.3–5.6 $Mg\,ha^{-1}\,year^{-1}$ of AGB loss from tree mortality (Chave et al., 2003). In line with this, estimates based on forest inventory plot data from the Central Amazon suggest that crown and partial trunk loss amounts to 0.9 $Mg\,ha^{-1}\,year^{-1}$ of dry mass litter production (Chambers et al., 2001; Chave et al., 2003).

Not all branch fall is due to damage, as trees routinely shed branches as they grow, a process referred to as branch turnover. Estimates of net primary productivity (NPP) to branch turnover range from 0.34 to 1.42 $Mg\,C\,ha^{-1}\,year^{-1}$ along a 3300m elevational transect in Peru (Malhi et al., 2017). Trees may also deliberately shed branches as a survival strategy during drought (Rood et al., 2000), or as a way to recover from liana infestation (Newbery & Zahnd, 2021). The ecological outcomes of branch loss from endogenous factors versus external factors may be quite different, as branch turnover can increase survival, whereas branch loss from damage is expected to reduce survival. Distinguishing between these two processes in the field is extremely challenging. However, remote sensing studies such as Araujo et al. (2021) described above sense the upper canopy, whereas branch turnover usually occurs in lower branches.

Crown damage is not routinely represented in vegetation demographic models, leading to potential biases in model predictions. While it is typical to account for leaf turnover (and in some cases branch biomass turnover, for example (Martínez Cano et al., 2020]) models that include crown area allometry typically assume that height, biomass, and crown area are directly related to stem diameter without consideration of deviations due to damage or differential growth. When biotic and abiotic disturbances have been included in vegetation models, including, for example, insects (Dietze & Matthes, 2014; Jönsson et al., 2012), wind (Lagergren et al., 2012), and large grazers (Pachzelt et al., 2015), they have been found to have a substantial impact on tree growth and mortality, and thus

forest biomass. These representations have generally invoked a direct increase in mortality (e.g. Jönsson et al., 2012]) or changes to physiological processes such as reductions in hydraulic conductivity or increases in root and leaf turnover (Dietze & Matthes, 2014). Likewise, fire models typically represent mortality based on scorch height, without changing the canopy structure of surviving trees (Drüke et al., 2019). As far as we are aware, no previous models have explicitly represented crown damage as changes in individual tree canopy structure and allometry (e.g. crown area relative to trunk diameter).

Given that the intensity and frequency of many types of disturbance are expected to increase over the coming decades (McDowell et al., 2018), including a representation of the nonlethal effect of disturbance on forest structure may be critical for correctly capturing the effect of disturbance on forest dynamics and biomass. In general, we expect nonlethal effects to introduce lags between environmental drivers and individual recovery or death, and we expect that these lags could alter demographic rates, forest structure, and carbon turnover. Following severe drought, trees have been observed to survive years with reduced leaf and fine root area before death (Anderegg et al., 2013; Berdanier & Clark, 2016; Henkel et al., 2016; Herguido et al., 2016; Rowland et al., 2015). Trees defoliated by insects or broken by wind damage can have reductions in growth rates that last over a decade (Tanner et al., 2014; Uriarte et al., 2004). Given that damage can be widespread, especially following disturbances like insect invasion or cyclones, these differences in growth rates can affect regional estimates of net primary productivity (NPP) as well as changing forest structure in terms of stem density, and light levels through to the understory (Brokaw & Grear, 1991). Initial crown damage from environmental drivers can also lead to a disturbance cycle by creating light gaps, which favor structural parasites such as lianas and climbing bamboos. These species further damage tree crowns creating additional tree gaps (Reis et al., 2020).

Here, we introduce an explicit crown damage module into the Functionally Assembled Terrestrial Ecosystem Simulator (FATES) and evaluate whether a delay between disturbance and mortality alters demographic rates and biomass dynamics. Specifically, we ask: (1) How do lags between damage and mortality change dynamics relative to equivalent instant increases in mortality? (2) How does the introduction of damage change simulated growth and mortality rates? Introducing new functionality requires additional model complexity, and so it is important to understand under what conditions tree damage may require explicit representation in models such as FATES.

2 | MATERIALS AND METHODS

2.1 | Model description and new developments

The FATES is a size- and age-structured vegetation demographic model that simulates the dynamics of cohorts (FATES Development Team, 2020; Koven et al., 2020). Cohorts are groups of individual

trees of the same size and plant functional type (PFT), with each co-hort modeled as one representative individual. The functional traits that define PFTs interact with environmental drivers to drive physi-ological processes that determine cohort dynamics such as growth and mortality rates. Disturbance dynamics in FATES follow the ecosystem demography (ED) approach (Moorcroft et al., 2001), and ecosystem biophysics are based on CLM4.5 (Oleson et al., 2013). Canopy organization uses elements of the perfect plasticity approxi-mation (PPA) (Fisher et al., 2010; Purves et al., 2008), which assumes that tree crowns are perfectly plastic and will grow to fill all avail-able canopy space. FATES must run as a component of a 'host' land model, the part of a climate model that simulates the dynamics of the land surface. Currently, FATES can run with the Energy Exascale Earth System Mode (E3SM) Land Model (ELM) (E3SM Project , 2018) or the community land model (CLM) (Lawrence et al., 2019). The PPA and ED components of FATES are described in Fisher et al. (2018). Recent FATES developments and benchmarking are described in Koven et al. (2020). The original CLM-ED model combining ED with elements of the PPA is described in Fisher et al. (2015).

2.2 | Representation of crown damage in FATES

To represent crown damage in FATES, we introduce a new crown damage module, in which damage is represented as a reduction in crown area and biomass of leaves, reproductive tissues, sapwood, storage, and structural pools. We reduce sapwood, storage, and structural biomass in proportion to the expected proportion of bio-mass in branches, assuming that storage carbon is distributed evenly among leaves, branches, the main stem, and roots (Hartmann & Trumbore, 2016). In our implementation, damage does not reduce the biomass of the main stem.

FATES is a cohort-based model, which means that plants with sim-ilar properties are grouped together and considered a single entity in the calculation of biophysical and ecological dynamics for computa-tional tractability. As these cohorts grow and die, they are dynami-cally fused and split over time, based on their similarity across a small number of either continuous or categorical dimensions. The essence of the ED-based approach described in Moorcroft et al. (2001) is to define two key continuous dimensions—plant size and the age since disturbance of the area the plant is occupying—that define the essential properties of a cohort. A third dimension is the plant functional type (PFT), which is categorical such that every cohort is associated with one of the distinct PFTs that comprise a simulation, and cohorts of different PFTs can never be fused. The coupling of ED with PPA (Purves et al., 2008) described in Fisher et al. (2015) adds a fourth dimension of discrete canopy strata that every cohort is assigned into based on their canopy height and crown area. This splitting of cohorts into distinct canopy strata allows for the repre-sentation of height-based light competition. These four dimensions uniquely define a cohort. Following growth, cohorts that are the same PFT and canopy layer, and within a specified DBH threshold of each other, are fused together to limit the number of cohorts that

need to be tracked. If, following growth, the crowns of cohorts in the canopy exceed patch area, some fraction of the smallest cohort (deterministic PPA) or all cohorts (stochastic PPA) will be demoted to the understory canopy layer (Figure S1) (see also Fisher et al., 2010; Koven et al., 2020). Understory cohorts receive less light than can-opy cohorts, and thus they have slower growth rates.

To model damage explicitly, we introduce a new fifth dimension to categorize cohorts, which we term 'damage classes'. During fu-sion, only cohorts of the same damage class can be fused. In simula-tions here, we use five damage classes, corresponding to 0, 20, 40, 60, and 80% loss of crown biomass. We also test the sensitivity of results to the number of crown damage classes. In FATES, the target size of various plant organs and tissues (leaves, roots, etc.) are given by allometric relationships with DBH. When damage occurs, it de-creases the biomass and target allometries of tissues in the crown, meaning that cohorts will remain at that damage level until carbon is available for recovery to a lower damage level (described below). The timing of damage events can be specified by the FATES user, for ex-ample to correspond to historic events such as cyclones. In the initial implementation of this module, we set damage to occur on the first day of each year. New damage is independent of previous damage (i.e. the same fraction of all cohorts gets damaged during each dam-age event) and the damaged fraction of each cohort gets split evenly into all higher damage classes (Figure 1b). This implementation limits the number of assumptions about the distribution of damage and corresponds to a representation of damage as a continuous back-ground process.

We implemented an explicit damage-dependent mortality term to capture the role of elevated mortality from damage due to pro-cesses not represented in FATES, such as increased vulnerability to pathogens and wind damage. Annual mortality from damage (m_d) is represented as a logistic function of crown loss,

$$m_d = \frac{1}{(1 + exp(-r(d-p)))} \tag{1}$$

Here, d is the proportion of crown loss; r is a rate parameter for the mortality increase with damage, here $r = 5.5$; and p is the inflection point parameter which sets the degree of damage over which mortality increases, here $p = 0.9$. Values for r and p were selected based on visual inspection of the logistic function fit to observations (Figure S2).

2.3 | Recovery dynamics

Recovery from damage occurs daily during the allocation of NPP to various tissues and involves a trade-off between DBH growth and regrowth of branches and leaves. In the existing FATES allocation scheme, NPP is first used to replace leaves and fine roots lost to turnover, and to bring storage carbon up to its allometric target. Any remaining carbon is then used to grow carbon pools that are below their specified target allometries. If any carbon is still remaining (car-bon balance, denoted Cb), it is used to grow all carbon pools and
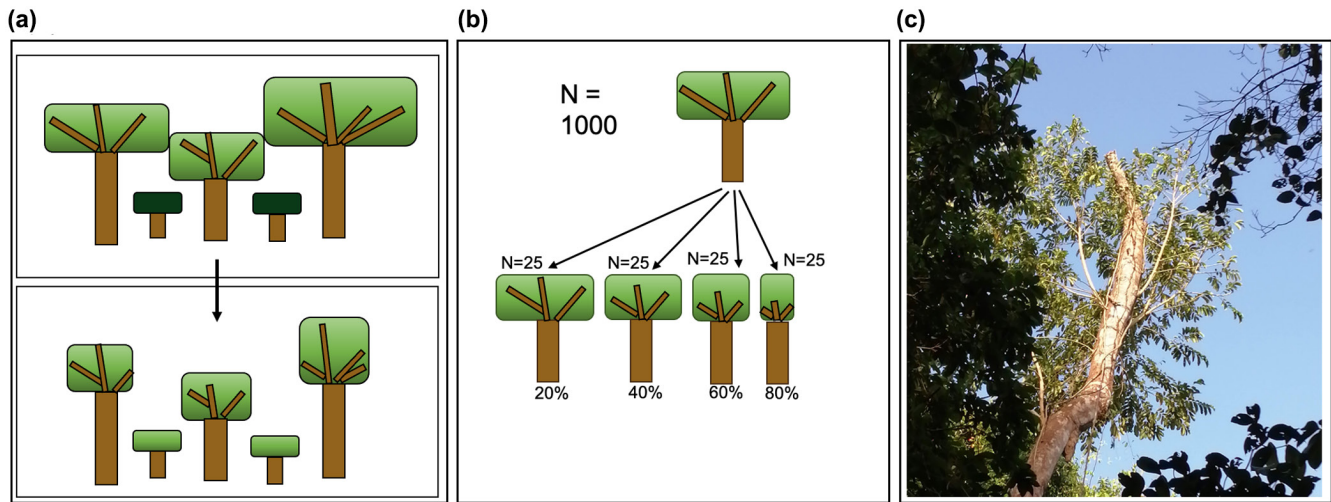
FIGURE 1 Schematic of crown damage implementation in FATES. (a) Crown damage results in a reduction in leaf, sapwood, storage, and structural biomass pools as well as a reduction in crown area. Following crown damage, understory trees, shown in dark green, are promoted to the canopy so that the canopy area remains constant. (b) Cohorts consist of groups of trees of the same size and PFT, modeled as one representative individual. During crown damage, the cohort is split and a specified fraction of individuals move to higher damage classes. In the example in b) the original cohort had 1000 individuals, and the damage fraction is 10%, therefore 25 individuals are put into each new cohort. (c) A damaged tree in BCI, Panama. Photo credit Pablo Narváez. [Colour figure can be viewed at wileyonlinelibrary.com]

DBH concurrently along their allometric trajectories. In FATES, damage decreases the target allometries of tissues in the crown. During daily allocation, Cb can be used to either grow tissues along their current damaged allometries, or to increase tissue mass to the target allometries of the next damage class, dependent on a recovery scalar parameter f_r (Figure 2). The maximum number of individuals of a cohort that can recover in each timestep (n_{max}) is a function of the available allocatable carbon to grow with (C_b), and the change in carbon between damage class i and $i-1$ (C_r):

$$n_{max} = n_i {}^* Cb / Cr, \qquad (2)$$

where n_i is the initial number density of the cohort. Since damaged plants face a choice of how to allocate carbon between recovery and growth, we have introduced a parameter f_r that determines the fraction of a cohort's carbon expenditure allocated towards recovery, versus the fraction that is allocated towards growth within the current damage class. The number of plants that recover n_r, is then $n_{max} {}^* f_r$. This implementation gives us the flexibility to capture contrasting patterns of regrowth following damage; continuous DBH growth at the expense of regrowing the crown, or regrowth of the crown at the expense of DBH and height growth, which may depend on species or degree of damage.

More information is given in Methods S2.

2.4 | FATES simulations

We ran multiple simulations which are summarized in Table 1 and Table S1 and referred to in the text by number, for example s1 for simulation 1, and so on. All simulations were run with either one or

two broadleaf evergreen tropical PFTs. Simulations were spun up from bare ground and run for 500 years, with the exception of the two PFT simulations, which took longer to reach equilibrium and were run for 700 years. We used a parameter file based on ensemble members from Koven et al. (2020) that were further calibrated against forest inventory data at BCI (Condit et al., 2019) and leaf mass area data (Dickman et al., 2019).

2.4.1 | Lags between damage and mortality

To evaluate how damage changes dynamics, and how these changes compare with those resulting from equivalent increases in mortality, we compared four configurations of FATES (Table 1): a control simulation in which the damage module is off (C; s1); a damage only simulation with just crown damage but no additional mortality (D; s2); a mortality only simulation in which cohorts are assigned to damage classes and are subjected to damage related mortality (Equation 1), but without any reduction to crown area or canopy biomass (M; s3); and a damage plus mortality simulation with crown damage and the explicit damage related mortality term (D + M; s4). The annual rate of damage was 1% and recovery was off in these simulations.

2.4.2 | Sensitivity to recovery

To test how the recovery parameter (fr) affects competitive dynamics we ran a simulation with two PFTs in which PFTs differed only in their ability to recover from damage (s5). The damage rate was set to 1% year^{-1} and the recovery parameter (fr) was 0 and 1 in the
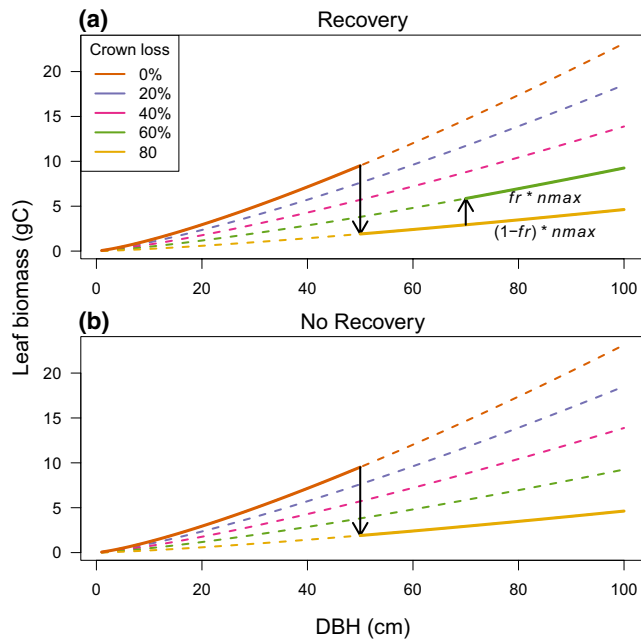
FIGURE 2 Schematic of recovery dynamics. Damage alters the target allometries of crown tissues (leaf, reproductive, sapwood, storage, and structural tissues; leaf tissues shown here as an example). Damage classes are shown with dashed lines. A damage event is shown with the first, downward arrow, which moves leaf biomass from 0% to 80% crown loss. (a) Initially the cohort grows along the new target allometry, but at some point it has excess carbon which it can use to grow a fraction of the cohort to the next damage class, shown with the second, upward arrow. n_{max} is the maximum number of individuals in the cohort that can recover to the next damage class with the available carbon. The parameter f_r determines the fraction of n_{max} that recovers to damage class 4 with 60% crown loss and the fraction that remains in damage class 5 with 80% crown loss. (b) If fr = 0, then there is no recovery and all individuals in the cohort remain with reduced allometries (in this example in damage class 5). [Colour figure can be viewed at wileyonlinelibrary.com]

two PFTs. One PFT therefore increases biomass of the canopy at the expense of DBH growth, increasing target allometries for a fraction of each cohort when available carbon allows. The other PFT uses available carbon to increase DBH and to grow canopy tissues along reduced allometric trajectories. To increase co-existence, this simulation was run with stochastic PPA, in which the demotion of cohorts from the canopy to the understory is not purely deterministic based on height. Rather, a fraction of all cohorts is demoted to the understory, with the fraction demoted depending on height, see Fisher et al. (2010).

2.4.3 | Carbon metabolism sensitivity

In FATES, we expected increases in mortality following crown damage to occur via carbon starvation mortality. Crown damage reduces both the photosynthesis and the respiration from the plant's canopy, while leaving stem and root respiration unchanged. If photosynthesis

is reduced so much that it cannot meet respiratory demand, storage carbon will be depleted, which triggers carbon starvation mortality in FATES. To investigate these dynamics, we tested the sensitivity of simulations to assumptions and parameters related to carbon storage and root respiration.

Root respiration is determined by the root nitrogen stoichiometry parameter, which has a default value of 0.03 gN/gC. An initial sensitivity analysis to the root nitrogen stoichiometry parameter suggested that carbon starvation mortality in trees with 80% crown loss increases sharply when root nitrogen stoichiometry reaches a critical value between 0.058 gN/gC and 0.066 gN/gC (Figure S3). At this level of root N stoichiometry, photosynthesis in damaged trees cannot match respiratory demands, leading to a depletion of storage carbon and carbon starvation mortality.

To compare dynamics when damage results in carbon starvation mortality, we therefore ran a control (s6) and a simulation with the damage module on (s7). In both simulations, we set root nitrogen stoichiometry to 0.66 gN/gC in order to increase respiratory demand. Further, in the damage simulation we reduced carbon storage in damaged trees, in proportion to crown loss, as this further increases the rate of carbon starvation mortality.

Additional crown damage classes come at a computational cost as FATES must track an increasing number of cohorts with each additional crown damage class. Yet, we expect that physiological responses to damage will depend on the degree of crown loss, and therefore a finer resolution of crown damage classes allows us to more fully capture the range of responses to damage. To explore this trade-off, we ran simulations with no damage, 2,3,4, and 5 crown damage classes. Since we expected the largest impact of damage on growth and mortality rates to be in trees with the most crown loss, we always included an 80% crown loss class. As we increased the number of damage classes, we added additional classes with lower levels of crown loss, Table S1.

For additional sensitivity analyses to carbon storage, damage rate and root nitrogen stoichiometry, see Methods S3.

2.5 | Benchmarking data

We compared FATES simulations to field data collected at Barro Colorado Island (BCI), Panama, between 2015 and 2019. The data were collected within a 50 ha permanent forest dynamic plot managed by the Smithsonian Tropical Research Institute and part of the Forest Global Earth Observatory (ForestGEO) (https://forestgeo.si.edu). Full censuses are carried out within the 50 ha plot approximately every 5 years, in which every stem ≥1 cm diameter at breast height (DBH, 1.3 m above the ground) is mapped, measured and identified to species level. The protocol for the full census is described in (Condit, 1998). In addition to the full census, damage and mortality surveys were conducted at BCI annually from 2016 to 2019. The protocol for damage and mortality surveys is described in (Arellano et al., 2021). Briefly, annual surveys followed a stratified sampling strategy in order to include a sufficient number of large trees. This involved sampling a sequence of nested and

TABLE 1 Model configurations

Simulation number	s1	s2	s3	s4	s5	s6	s7
Name	Control	Damage only	Mortality only	Damage + mortality	Two PFTs	High root N control	High root N damage
Root N stoichiometry	0.029	0.029	0.029	0.029	0.029	0.066	0.066
Damage	No	Yes	No	Yes	Yes	No	Yes
Carbon storage decrease with damage	-	No	-	No	No	-	Yes
m_d term (additional damage-driven mortality)	-	No	Yes	Yes	Yes	-	No
Damage rate (% year^{-1})	-	1	1	1	1	-	1
Recovery (f_r)	-	0	0	0	0, 1	-	0
PFTs	1	1	1	1	2	1	1
Allocation to storage	1.2	1.2	1.2	1.2	1.2	1.2	1.2
Stochastic PPA	No	No	No	No	Yes	No	No

increasingly smaller subplots, with a smaller DBH threshold for stem inclusion in smaller subplots. In total 8049 stems were assessed over the 4 years. In these surveys, stems are assessed as alive or dead, and coded as either standing, broken, or uprooted. For live stems, the main axis of the tree is identified as a continuous axis that includes the stem and the widest branch at each branching point to the top of the crown. The percentage of the main axis that is living tissue is estimated (henceforth, 'living length') and within the living length the fraction of branches remaining (b_l) is estimated based on signs of recent damage. We used both the living length and b_l to estimate the biomass of a living tree based on an allometric function that accounts for the vertical distribution of volume in the trunk vs. crown (Ver Planck & MacFarlane, 2014). Specifically, we estimated the proportion of crown volume below a given height (within the living length) and multiplied it by the relative biomass of the crown, which was set to 1/3 of the total biomass of the tree based on empirical data from 611 harvested tropical trees (Chambers et al., 2001; Duque et al., 2017), see (Zuleta et al., 2021, 2022), and Methods S3 for a full explanation. Based on estimated damage we grouped trees into five damage classes (corresponding to the damage classes used in FATES) and calculated mortality, M, for each class as

$$M_d = \left(\log(N_{1,d}) - \log(N_2)\right)/t, \tag{3}$$

where d is damage class, N_1 is the number of individuals alive in census 1, N_2 is the number of individuals alive in census 2 (regardless of damage class in census 2), and t is time in years between censuses. We excluded multi-stemmed trees from this analysis to avoid the influence of multiple stems on mortality rates. To account for the stratified sampling design, individuals were weighted by the frequency of their size class and species within the 50 ha plot relative to their frequency in the sample (following Zuleta et al. (2021)).

To benchmark growth rates, we compared FATES simulations with dendrometer band data collected at BCI from 1290 trees between 2015 and 2020 (Ramos et al., 2022). We used measurements collected annually in the late wet season to avoid influences of seasonal fluctuations in DBH. In the dendrometer data, crown illumination (CI) was assessed on a scale from 1 to 5 (Poorter et al., 2005), which we mapped onto FATES canopy layers by calling CI classes 4 and 5 canopy, and CI classes 1 and 2 understory. Trees in CI class 3 (between 245 and 318 across censuses) have 10–90% overhead light, and were therefore not included in this analysis as they do not correspond well with FATES canopy layers. Crown damage was assigned based on a visual assessment of the crown using a four-point scale (4 indicates 75%–100% of the crown is intact, 3 indicates 50%–75%, 2 indicates 25%–50%, and 1 indicates 0%–25%). To reduce the confounding effects of lianas on growth rates, we repeated the analysis excluding trees classified as having 50% liana cover.

We compared the canopy area damaged each year, and the ratio of mortality to damage canopy turnover from simulations with observations of branch fall from repeated drone measurements over BCI (from Araujo et al. (2021)). Tree size distributions were also compared with the full BCI census data, census interval 2010–2015 (Condit et al., 2019).

3 | RESULTS

3.1 | Effects of damage and mortality on canopy dynamics

AGB differed strongly between simulations with and without damage and mortality. AGB decreased from 18.5 kg m^{-2} in the control (C; s1) to 17.5 kg m^{-2} in the damage only simulation (D; s2), 13.1 kg m^{-2} in the mortality only simulation (M; s3) and 14.5 kg m^{-2} in the damage plus mortality simulation (D+M; s4) (Figure 3a). AGB at BCI is approximately 15.3 kg m^{-2} (Chave et al., 2008), closest to the damage plus mortality simulation under this parameterization.

Carbon residence time was calculated as total vegetation / NPP, as in Koven et al. (2015). Since NPP did not change significantly with damage, carbon residence time and AGB are roughly proportional to one another across simulations. Carbon residence time decreased the most in the mortality only simulation and least in the damage only simulation, relative to the control (Figure 3b).

Damage and mortality both cause changes to the canopy structure (Figure 3c). In all cases, the creation of gaps allows for understory trees to be promoted to the canopy. The minimum height for a cohort to be in the canopy (canopy height threshold or critical height) therefore decreased from 18.2 m in the control (s1) to 15.5 m in the damage only simulation (s2), 12.7 m in the mortality only simulation (s3) and 14.7 m in the damage plus mortality simulation (s4). These values bracket the estimated canopy height threshold at BCI of 16.4 m (Bohlman & Pacala, 2012), with the damage only simulation coming closest to observations under this parameterization. Neither
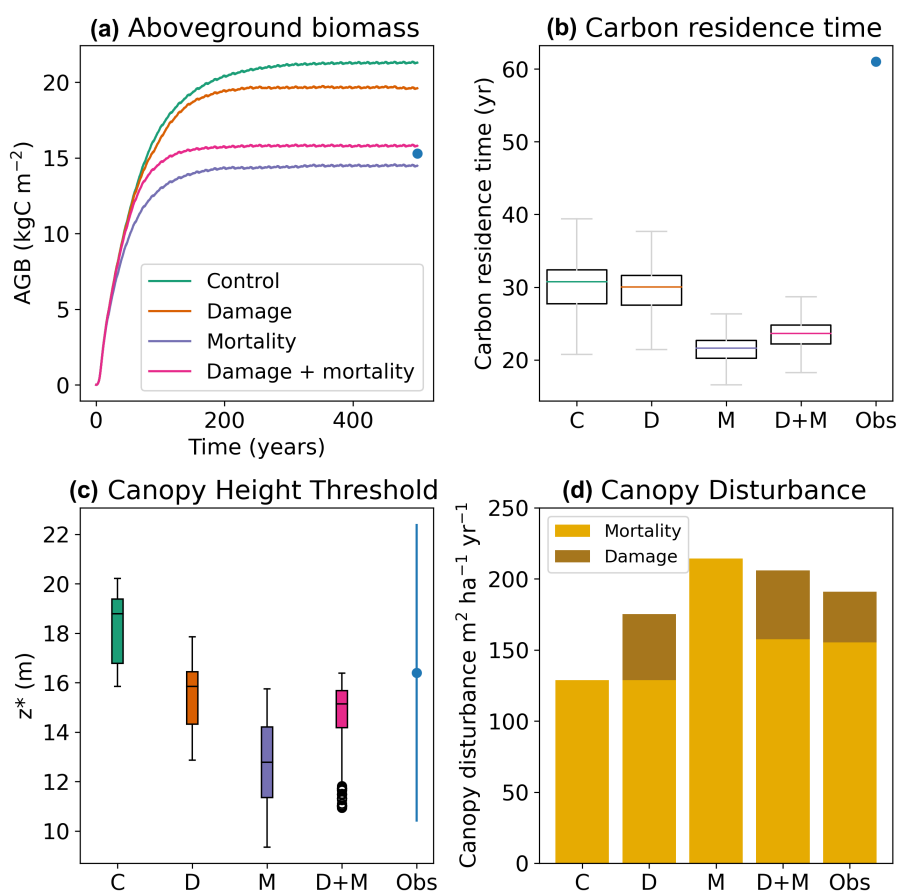

FIGURE 3 AGB, carbon residence time, canopy height threshold and canopy disturbance. The control simulation (C; s1) has the damage module turned off. The damage simulation (D; s2) has crown damage turned on—that is, cohorts lose crown area and canopy biomass. In the mortality simulation (M; s3), cohorts are split into damage classes and are subjected to damage related mortality but do not have any reduction in crown area or canopy biomass. In the damage + mortality simulation (D+M; s4), cohorts have both crown damage and damage related mortality. (a) AGB is lowest in M (s3) because mortality affects trees with full crowns, whereas in D+M (s4) increases in mortality are in damaged trees. AGB at BCI is estimated at 15.3 kg m^{-2}, shown in blue (Chave et al., 2008). (b) Carbon residence times in the last 100 years of the simulations vary among scenarios in proportion to AGB. Boxes show the interquartile range, whiskers extend to 1.5 x the interquartile range. Outliers are not shown. Carbon residence time at BCI is estimated at 61 years, shown in blue (Chave et al., 2008). (c) Height threshold for a cohort being in the canopy in patches over 50 years, over the last 100 years of the simulation. Damage causes understory trees to be promoted to the canopy at smaller heights, leading to a decrease in the number of large trees in the understory, and a decrease in the canopy height threshold. The mean canopy height threshold at BCI is estimated to be 16.4 m (sd 6.02 m) (Bohlman & Pacala, 2012), shown in blue. (d) Shows the area of canopy disturbance by mortality and damage (in simulations with damage—D and D+M) and in observations from drone measurements over BCI from Araujo et al. (2021). [Colour figure can be viewed at wileyonlinelibrary.com]

damage nor mortality have much effect on the overall size-structure of the forest (Figure S4). In all simulations, the number of very small and very large trees is underestimated relative to observations.

Araujo et al. (2021) analyzed monthly drone images over the 50 ha plot at BCI between 2017 and 2019 and found that of the total disturbed area of 23,289 m^2 (155.3 m^2 year^{-1} ha^{-1}), 23% was attributed to branch fall rather than mortality (35.7 m^2 year^{-1} ha^{-1}). In our damage plus mortality simulation (s4), 28% of total disturbed area is due to canopy damage, and the total disturbed area is overestimated at 177.2 m^2 year^{-1} ha^{-1}. The damage only simulation (s2) has a total disturbed area of 175.2 m^2 year^{-1} ha^{-1}, of which 26% was due to canopy damage. Total disturbed area is slightly underestimated in the control simulation (s1) at 128.8 m^2 year^{-1} ha^{-1}, and overestimated in the mortality only simulation (s3) at 214.3 m^2 year^{-1} ha^{-1}.

3.2 | Effects of crown damage on demographic rates

We expected that crown damage would increase mortality and decrease growth rates. Observations from the damage and mortality surveys at BCI show a clear increase in mortality with increasing crown damage, but only in understory trees. This pattern is captured in FATES simulations with high root N stoichiometry and reductions in storage carbon (s7). In this configuration, photosynthesis in damaged trees is not

sufficient to meet high respiratory demand from roots, leading to a depletion of storage carbon and an increase in carbon starvation mortality with damage (Figure 4). In simulations with low root N stoichiometry and no reduction in carbon storage with damage (s4), carbon starvation only increased in understory trees with 80% crown loss and total mortality is underestimated compared with observations.

In the damage-only simulation with low root respiration (D; s2), DBH increments of canopy trees are a good fit to dendrometer band data at BCI, apart from being slightly underestimated in high damage classes (Figure 5a). DBH growth rates in understory cohorts are underestimated compared with observations from BCI, but capture the trend of decreasing growth with increasing damage. In high root N simulations, s7, the trend of decreasing growth rates with increasing crown loss matches observations from BCI, but canopy DBH growth rates are slightly underestimated, and understory DBH growth rates are underestimated across crown damage classes (Figure 5b). Due to increased root N stoichiometry, root respiration is higher in these simulations than in previous FATES cases (e.g. Koven et al. (2020)), and thus, it is likely that compensating errors may exist in the carbon balance of understorey plants. In both sets of simulations low NPP or high maintenance respiration may be contributing to the mismatch between simulated and observed understory growth rates. Observed growth rates of canopy and understory trees are higher when trees with high liana load are excluded from the BCI data (Figure S5).
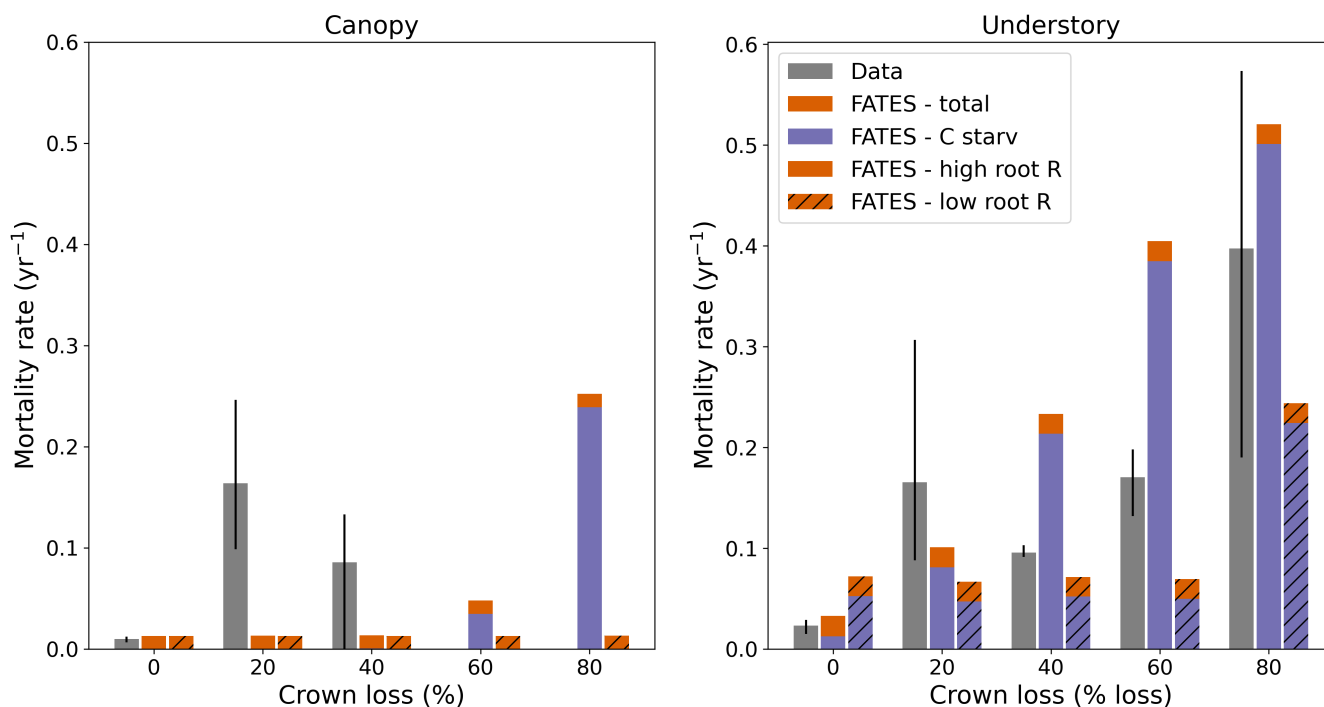

FIGURE 4 Annual mortality rate by damage class and canopy layer. Gray bars show mean mortality by damage class for all trees >1 cm dbh, based on damage and mortality surveys conducted annually at BCI over three years. Error bars show the range of mean mortality by damage across census intervals. Solid orange and purple bars show the total mortality and carbon starvation mortality by damage in FATES simulation s7, in which carbon storage is reduced in damaged trees and root respiration is high. In this configuration mortality is overestimated compared with observations in high damage classes. Hatched bars show mortality in FATES simulation s2, in which carbon storage is not reduced in damaged trees and root respiration is lower. In this configuration mortality of trees with high damage is underestimated compared with observations, especially in the understory. [Colour figure can be viewed at wileyonlinelibrary.com]
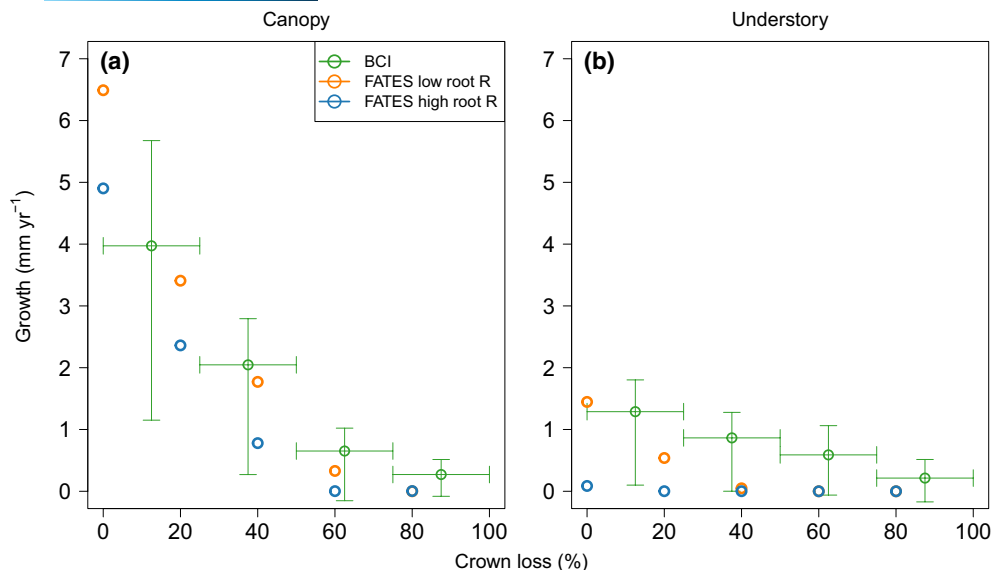
FIGURE 5 Annual DBH growth rate by damage class and canopy layer in FATES simulations and observations from BCI. Orange circles show the low root N configuration of FATES (s2) and blue circles show the high root N configuration of FATES (s7). Green lines show growth rates from dendrometer band data at BCI, divided into canopy and understory. Error bars show the 50th percentile of growth rates across five census intervals. Note that damage classes in the observations are different than in FATES simulations, and hence points are offset. Damage classes in the observations include trees with a range of crown loss shown with horizontal lines, whereas in FATES damage classes correspond to a fixed percentage of crown loss. In the low root N configuration canopy growth rates are a good fit to data, and understory growth rates are slightly underestimated. With high root N, simulated growth rates of canopy trees slightly underestimate observations from BCI and simulated understory growth rates are extremely low. See Figure S5 for a version of this figure in which trees in BCI with >50% liana load were excluded. [Colour figure can be viewed at wileyonlinelibrary.com]
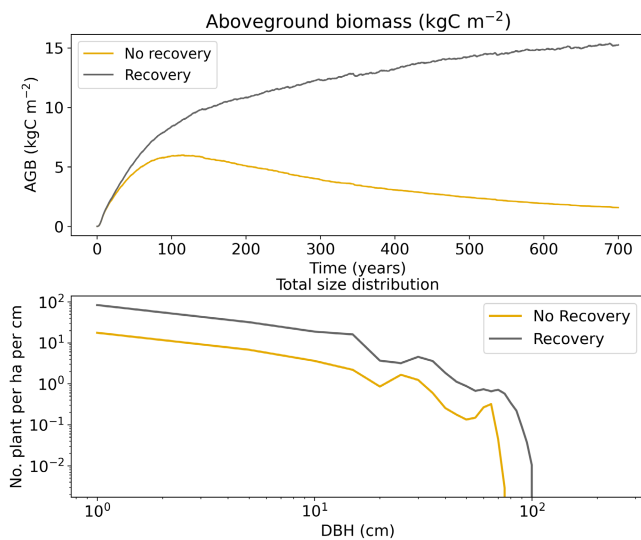

FIGURE 6 AGB and size-distribution of two PFT simulations in the low root N configuration (s5). In the two PFT simulations, PFTs are identical except for the recovery scalar parameter which is 0 in the 'no recovery' PFT and 1 in the 'recovery' PFT. The PFT that is able to recover out-competes the no recovery PFT. [Colour figure can be viewed at wileyonlinelibrary.com]

3.3 | Competition between PFTs that differ in ability to recover from damage

In the two PFT simulation (s5) in which PFTs differ only in the recovery parameter (f_r), the recovery PFT dominates in terms of AGB from

year 50 onwards (Figure 6) and accounts for 90% of plot AGB after 700 years. DBH growth rates are temporarily lower in the recovery PFT as carbon is used to regrow the canopy (Figure S6). However, once trees recover they have faster DBH growth rates and ultimately outcompete the nonrecovery trees.

4 | DISCUSSION

Crown damage and damage-driven mortality are important processes shaping forest structure and response to disturbance. Despite this, crown damage is rarely represented in vegetation models. We introduce a crown damage module into the vegetation demographic model FATES and find that damage itself alters demographic rates, the canopy structure of the forest, and the competitive dynamics of PFTs.

4.1 | The effects of damage on carbon starvation mortality are sensitive to the ratio of leaf to stem and root respiration and the impacts of damage on storage

We expected that crown damage would alter demographic rates, increasing mortality and decreasing growth rates. We find that the degree to which crown damage results in increases in carbon starvation mortality is highly dependent on model configuration. Carbon starvation mortality occurs in FATES when stored carbon is less than

the allometric target leaf carbon for a given DBH. If the stored carbon pool is reduced when trees are damaged then the conditions for carbon starvation are more frequently met. This is exacerbated when root and stem respiration are high relative to photosynthesis. Following damage, photosynthetic capacity is reduced. In order to meet respiratory demand from remaining undamaged tissues with limited photosynthetic capacity, damaged trees deplete their stored carbon pool, triggering carbon starvation mortality. When we configure FATES with both reductions in stored carbon and a high ratio of root and stem to leaf respiration, we find that carbon starvation mortality increases in understory trees in line with observed increases in mortality with damage. Carbon starvation mortality in canopy trees is overestimated under this configuration. In contrast, when storage carbon is not reduced in damaged trees, and the ratio of root and stem to leaf respiration is low, damage leads to small increases in carbon starvation mortality, and only in severely damaged, small trees.

An improved understanding of allocation and storage in damaged trees, as well as data on stem and root respiration rates, could help to constrain the representation of damage and recovery in FATES. Carbon storage is often estimated by measuring the concentration of nonstructural carbohydrates (NSCs). NSCs have a broad range of functions in trees including acting as a buffer between carbon supply and demand and maintaining hydraulic integrity, (see (Hartmann & Trumbore, 2016)). Defoliated trees have been found to increase the concentration of NSCs in their tissues, possibly to increase their safety margins in the face of uncertain future environments (Sala et al., 2012). New approaches to quantify NSC dynamics over a range of timescales are providing new insights into the role of stored carbon in regulating tree response to environmental stress (Blessing et al., 2015) and could help inform how we represent the physiological response to crown damage in vegetation models.

We find that carbon starvation mortality in the model results when root and stem respiration outpace carbon acquisition. In reality, experiments suggest that allocation to root biomass is reduced following defoliation, in order to maintain carbon balance (Eyles et al., 2009; Stevens et al., 2008). If damaged trees are also likely to reduce their root biomass (especially of active tissues) following damage, they may be able to limit carbon starvation mortality. This scenario is more similar to our low root N simulations, in which damage does not lead to an increase in carbon starvation mortality. Allometric optimization under a range of environmental conditions is a large field of research (Dybzinski et al., 2011; Farrior et al., 2013; Trugman et al., 2018), and future work will focus on investigating the impacts of different allocation strategies on recovery and mortality following damage.

It is likely that some combination of mechanisms including, but not limited to, carbon starvation mortality are responsible for observed increases in mortality with damage. Damage can create entry points to pathogens or make a tree vulnerable to windthrows (Taylor & MacLean, 2009), while droughted trees with crown dieback may frequently die of hydraulic failure rather than carbon starvation mortality (Adams et al., 2017; McDowell et al., 2008; McDowell & Sevanto, 2010; Rowland et al., 2015). The optional damage-dependent mortality term introduced in the crown damage module is designed to capture the increased risk of mortality in damaged trees by mechanisms not represented in FATES.

4.2 | Crown damage decreases growth rates

Under all configurations of FATES, crown damage decreased diameter growth rates. It is estimated that 15–45% of aboveground woody productivity is replacement of branch loss (Gora et al., 2019; Malhi et al., 2014; Marvin & Asner, 2016), although some portion of this is branch turnover rather than tree damage. In our simulations, the degree to which NPP is used for replacement of branches versus diameter increment is determined by the recovery scalar parameter. When recovery is high, we see a reduction in diameter growth rates in the heavily damaged trees, as NPP is used to replace branches and leaves. When recovery is low, NPP is used for diameter growth, at the expense of regrowing the canopy. This approach allows us to capture contrasting patterns of growth observed in damaged trees. For instance, following severe drought damaged trees can continue to grow radially for several years until death (Anderegg et al., 2013; Rowland et al., 2015). This paradoxical observation can be explained by carbon allocation optimality models that suggest trees must prioritize repair of damaged xylem vessels in order to recover, especially under dry conditions (Trugman et al., 2018). In other studies of drought-damaged trees, and in hurricane-damaged trees, reduced growth rates have been observed for over 10 years (Berdanier & Clark, 2016; Tanner et al., 2014). Reduced growth rates following disturbance can compound (Umaña & Arellano, 2021) with negative implications for the forest carbon budget (Yang et al., 2018). As we link the crown damage module in FATES to explicit drivers and physiological mechanisms of mortality, we will test how different rates of recovery impact mortality and competitive dynamics.

4.3 | Lags between damage and mortality

We also expected that lags between damage and mortality would alter dynamics relative to equivalent instant increases in mortality, that is, simulations with a damage-dependent mortality term but no reduction in crown biomass or crown area. The crown damage module leads to smaller decreases in AGB and carbon residence time than equivalent instant increases in mortality. Damage results in a loss of biomass from damaged trees, but there is a compensatory effect whereby smaller crowns allow more trees to fit into the canopy where they have faster growth rates. Although the net effect of damage is still a decrease in AGB, the decrease is not as large as when all biomass is lost instantly as in the mortality only simulation.

There are trade-offs when adding new functionality to a model like FATES between improved predictive capabilities and increased computational costs, along with additional process and parametric uncertainty. This is our first exploration of these trade-offs using

the crown damage module in FATES. We compared these first simulations against data from BCI, a tropical forest that historically has not been subject to catastrophic disturbance. In these simulations, it is not clear that the damage module leads to a significantly better fit to observations than simulations with an equivalent instant increase in mortality. However, a more realistic representation of disturbance may be important in other cases. Disturbances are critical for explaining forest size distributions (Farrior et al., 2016) and have important implications for successional dynamics, as increased light levels in the understory favor fast-growing light-demanding species (Brokaw, 1987). Given that a significant proportion of canopy turnover is attributed to disturbance-driven crown damage (Araujo et al., 2021; Chambers et al., 2001), representing this process is important for correctly estimating size distributions, and the impact of canopy gaps on recruitment and succession. Further, periodic, severe disturbances can cause high levels of defoliation and branch loss (Liu et al., 2018) with impacts that can last for months (Lodge et al., 1991). In future work, we will therefore test how higher rates of crown damage influence forest recovery following large-scale disturbance.

In the sensitivity analysis to the number of crown damage classes, we find that it is the inclusion of severely damaged trees (80% crown loss) that most impact forest dynamics (Figure S7). Including additional damage classes with lower rates of crown loss did not change dynamics relative to simulations, which only included undamaged and severely damaged trees. Since having fewer damage classes limits the number of cohorts that need to be simulated, this significantly reduces the computational cost of simulations. Simulations with just two damage classes were 20% slower than the control run with the damage module off, whereas simulations with five damage classes were 84% slower than the control. Given these results, we recommend that the damage module only be used in areas of high disturbance, and only with two damage classes to simulate undamaged, and highly damaged cohorts.

4.4 | The ability to recover from damage alters successional dynamics

Differences in the ability to tolerate and recover from crown damage is another axis of variation that determines PFT response to disturbance and successional dynamics. We find that PFTs with the ability to recover outcompete PFTs with no recovery (which never regrow back to the default allometry) despite the short term decrease in DBH growth rates. In these simulations, PFTs differed only in their recovery ability, but it is likely that a suite of functional traits will determine both susceptibility to damage and the ability to recover (Hogan et al., 2018; Paz et al., 2018; Uriarte et al., 2004). For example, higher wood density and lower specific leaf area (SLA) were associated with lower rates of damage in an Australian rainforest following Tropical Cyclone Larry (Curran et al., 2008). Single PFT simulations using FATES were able to reproduce LANDSAT observations of biomass recovery from windthrow at a site in the Central Amazon (Negrón-Juárez et al., 2020). However, to capture observed

changes in functional composition in response to disturbance, it will be necessary to simulate multiple PFTs that differ in traits determining susceptibility to and recovery from disturbance, for instance leaf water potentials and wood density (Powell et al., 2018). Identifying relevant trade-offs relating to disturbances and competitive dynamics and the underlying functional traits will be key to understanding both the dynamics of co-existence, and also how changes to disturbance frequency and severity will alter future community composition (Flake et al., 2021; Powell et al., 2018).

4.5 | Linking damage to specific environmental drivers will allow interactions between disturbances

Interactions between disturbances may alter final mortality rates via their effects on crown condition, and these effects may be difficult to capture in vegetation models unless crown damage is explicitly modeled. Many types of disturbance are predicted to increase in either frequency and or intensity, including droughts (Trenberth et al., 2013), wildfires (Westerling et al., 2011), pest and pathogen outbreaks (Seidl et al., 2018), cyclones (Balaguru et al., 2018), and anthropogenic disturbance (Hurtt et al., 2020). These disturbances often overlap spatially and temporally, with compounding impacts on mortality rates. For instance, a severe drought may not kill a tree, but might make it more susceptible to death from another source such as insects (Anderegg et al., 2015; Gaylord et al., 2013), wind damage (Csilléry et al., 2017) or future droughts (Anderegg et al., 2013). In southeastern Amazonia, intensification of the dry season has led to an increase in wildfires, resulting in the forest there transitioning from a carbon source to a carbon sink (Gatti et al., 2021). In current models, these synergistic stresses aren't resolved, and are instead aggregated into a constant background mortality term that is likely under-responsive to changes in disturbance regimes and environmental conditions. Tracking damage in vegetation models enables a representation of the legacy of previous stresses and the ways that disturbances compound to drive regional patterns of mortality. Future work will focus on linking crown damage with environmental drivers and testing the sensitivity of mortality to changes in disturbance regimes.

5 | CONCLUSIONS

We introduced a crown damage module into FATES, enabling us to test the impact of event-based crown damage on forest size structure and carbon cycling dynamics. Crown damage leads to decreases in AGB and carbon residence time, as well as decreases in the canopy height threshold. Comparing these simulations with versions without damage but with equivalent increases in mortality, we find that decreases in AGB and carbon residence time are largely due to increased mortality. Nevertheless, decreases in growth rates of damaged trees alter the competitive dynamics of PFTs, with PFTs that are able to recover crown biomass outcompeting those that are

not. Linking the crown damage module with environmental drivers of damage and physiological mechanisms of death will further our understanding of how forests will respond to a changing climate and altered disturbance regimes.

AUTHOR CONTRIBUTIONS

JFN and CDK designed the research. JFN carried out the research. RGK, CDK, and RAF are among the principal developers of FATES and helped with implementation of new features and interpretation of simulation results. GA, DZ, SD, and DM collected and contributed the damage and mortality survey data and aided with the interpretation of the data. HML contributed the BCI dendrometer data and aided with the interpretation of the data. VH helped with analysis of dendrometer band data. JFN wrote the initial draft of the manuscript, and all authors contributed comments and helped with revision of the manuscript.

CONFLICT OF INTEREST

The authors declare no competing interests.

DATA AVAILABILITY STATEMENT

FATES outputs can be accessed at https://ngt-data.lbl.gov/dois/NGT0187/

Needham, J., Arellano, G., Davies, S., Fisher, R., Hammer, V., Knox, R., Mitre, D., Muller-Landau, H. C., Zuleta, D., & Koven, C. (2022). FATES crown damage simulation outputs 2022. 1.0. NGEE Tropics Data Collection. (dataset). https://doi.org/10.15486/ngt/1871026

Python and R scripts for analysing the data and reproducing the figures in this manuscript at https://github.com/JessicaNeedham/Needham_etal_GCB_2022_FATES_crown_damage.

All FATES source code is available at https://github.com/NGEET/fates. Commits used in simulations here are on JFN's fork of the main FATES repository. High carbon starvation mortality configurations use commit 354f0b0c, low carbon starvation mortality configurations use commit bf013ef, and low carbon starvation

mortality with mortality only use commit ef845c8, all from the branch JessicaNeedham-damage_recovery found here: https://github.com/JessicaNeedham/fates/tree/JessicaNeedham-damage_recovery

The sensitivity to the number of crown damage classes used commit 8f994c2 on the branch JessicaNeedham-crowndamage_module found here: https://github.com/JessicaNeedham/fates/tree/JessicaNeedham-crowndamage_module

Damage and mortality surveys from BCI are available upon request from S.J.D., D.Z. and G.A. and the PIs of the BCI forest dynamics plot.

BCI dendrometer data are available at https://smithsonian.figshare.com/

Ramos, Pablo, Paulino Villareal, Richard Condit, KC Cushman, and Helene C. Muller-Landau. 2022. Annual dendrometer data from the Barro Colorado Island 50-ha forest dynamics plot for 2015–2020. Smithsonian Figshare. DOI 10.25573/data.19985066

Full BCI census data are available from.

Condit, Richard et al. (2019), Complete data from the Barro Colorado 50-ha plot: 423617 trees, 35 years, Dryad, Dataset, https://doi.org/10.15146/5xcp-0d46

ORCID

Jessica F. Needham https://orcid.org/0000-0003-3653-3848
Rosie A. Fisher https://orcid.org/0000-0003-3260-9227
Ryan G. Knox https://orcid.org/0000-0003-1140-3350

REFERENCES

Adams, H. D., Zeppel, M. J. B., Anderegg, W. R. L., Hartmann, H., Landhäusser, S. M., Tissue, D. T., Huxman, T. E., Hudson, P. J., Franz, T. E., Allen, C. D., Anderegg, L. D. L., Barron-Gafford, G. A., Beerling, D. J., Breshears, D. D., Brodribb, T. J., Bugmann, H., Cobb, R. C., Collins, A. D., Dickman, L. T., … McDowell, N. G. (2017). A multispecies synthesis of physiological mechanisms in drought-induced tree mortality. *Nature Ecology and Evolution*, 1(9), 1285–1291.

Anderegg, W. R. L., Hicke, J. A., Fisher, R. A., Allen, C. D., Aukema, J., Bentz, B., Hood, S., Lichstein, J. W., Macalady, A. K., McDowell, N., Pan, Y., Raffa, K., Sala, A., Shaw, J. D., Stephenson, N. L., Tague, C., & Zeppel, M. (2015). Tree mortality from drought, insects, and their interactions in a changing climate. *The New Phytologist*, 208(3), 674–683.

Anderegg, W. R. L., Plavcová, L., Anderegg, L. D. L., Hacke, U. G., Berry, J. A., & Field, C. B. (2013). Drought's legacy: Multiyear hydraulic deterioration underlies widespread aspen forest die-off and portends increased future risk. *Global Change Biology*, 19(4), 1188–1196.

Araujo, R. F., Grubinger, S., Celes, C. H. S., Negrón-Juárez, R. I., Garcia, M., Dandois, J. P., & Muller-Landau, H. C. (2021). Strong temporal variation in treefall and branchfall rates in a tropical forest is explained by rainfall: Results from five years of monthly drone data for a 50-ha plot. *Biogeosciences*, 18(24), 6517–6531.

Arellano, G., Medina, N. G., Tan, S., Mohamad, M., & Davies, S. J. (2019). Crown damage and the mortality of tropical trees. *The New Phytologist*, 221(1), 169–179.

Arellano, G., Zuleta, D., & Davies, S. J. (2021). Tree death and damage: A standardized protocol for frequent surveys in tropical forests. *Journal of Vegetation Science*, 32(1), e12981. https://doi.org/10.1111/jvs.12981

Balaguru, K., Foltz, G. R., & Leung, L. R. (2018). Increasing magnitude of hurricane rapid intensification in the central and eastern tropical Atlantic. *Geophysical Research Letters*, 45, 4238–4247. https://doi.org/10.1029/2018GL077597

Berdanier, A. B., & Clark, J. S. (2016). Multiyear drought-induced morbidity preceding tree death in southeastern U.S. forests. *Ecological Applications*, 26(1), 17–23.

Blessing, C. H., Werner, R. A., Siegwolf, R., & Buchmann, N. (2015). Allocation dynamics of recently fixed carbon in beech saplings in response to increased temperatures and drought. *Tree Physiology*, 35(6), 585–598.

Bohlman, S., & Pacala, S. (2012). A forest structure model that determines crown layers and partitions growth and mortality rates for landscape-scale applications of tropical forests. *Journal of Ecology*, 100(2), 508–518.

Brokaw, N. V. L., & Grear, J. S. (1991). Forest structure before and after hurricane Hugo at three elevations in the Luquillo mountains, Puerto Rico. *Biotropica*, 23(4), 386.

Brokaw, N. V. L. (1987). Gap-phase regeneration of three Pioneer tree species in a tropical Forest. *Journal of Ecology*, 75(1), 9.

Carnicer, J., Coll, M., Ninyerola, M., Pons, X., Sánchez, G., & Peñuelas, J. (2011). Widespread crown condition decline, food web disruption, and amplified tree mortality with increased climate change-type drought. *Proceedings of the National Academy of Sciences of the United States of America*, 108(4), 1474–1478.

Chambers, J. Q., Santos, J. d., Ribeiro, R. J., & Higuchi, N. (2001). Tree damage, allometric relationships, and above-ground net primary production in Central Amazon forest. *Forest Ecology and Management*, 152(1–3), 73–84.

Chave, J., Condit, R., Lao, S., Caspersen, J. P., Foster, R. B., & Hubbell, S. P. (2003). Spatial and temporal variation of biomass in a tropical forest: Results from a large census plot in Panama. *Journal of Ecology*, 91(2), 240–252.

Chave, J., Condit, R., Muller-Landau, H. C., Thomas, S. C., Ashton, P. S., Bunyavejchewin, S., Co, L. L., Dattaraja, H. S., Davies, S. J., Esufali, S., Ewango, C. E. N., Feeley, K. J., Foster, R. B., Gunatilleke, N., Gunatilleke, S., Hall, P., Hart, T. B., Hernández, C., Hubbell, S. P., … Losos, E. C. (2008). Assessing evidence for a pervasive alteration in tropical tree communities. *PLoS Biology*, 6(3), e45.

Condit, R. (1998). The CTFS and the standardization of methodology. In *Tropical Forest Census Plots* (pp. 3–7). Springer Berlin Heidelberg.

Condit, R., Pérez, R., Aguilar, S., Lao, S., Foster, R., & Hubbell, S. (2019). Complete data from the Barro Colorado 50-ha plot: 423617 trees, 35 years, Dryad, Dataset. https://doi.org/10.15146/5xcp-0d46

Csilléry, K., Kunstler, G., Courbaud, B., Allard, D., Lassègues, P., Haslinger, K., & Gardiner, B. (2017). Coupled effects of wind-storms and drought on tree mortality across 115 forest stands from the Western Alps and the Jura mountains. *Global Change Biology*, 23(12), 5092–5107.

Curran, T. J., Brown, R. L., Edwards, E., Hopkins, K., Kelley, C., McCarthy, E., Pounds, E., Solan, R., & Wolf, J. (2008). Plant functional traits explain interspecific differences in immediate cyclone damage to trees of an endangered rainforest community in North Queensland. *Austral Ecology*, 33(4), 451–461.

Dickman, L. T., McDowell, N. G., Grossiord, C., Collins, A. D., Wolfe, B. T., Detto, M., Wright, S. J., Medina-Vega, J. A., Goodsman, D., Rogers, A., Serbin, S. P., Wu, J., Ely, K. S., Michaletz, S. T., Xu, C., Kueppers, L., & Chambers, J. Q. (2019). Homoeostatic maintenance of nonstructural carbohydrates during the 2015–2016 El Niño drought across a tropical forest precipitation gradient. *Plant, Cell and Environment*, 42(5), 1705–1714.

Dietze, M. C., & Matthes, J. H. (2014). A general ecophysiological framework for modelling the impact of pests and pathogens on forest ecosystems. *Ecology Letters*, 17(11), 1418–1426.

Drüke, M., Forkel, M., von Bloh, W., Sakschewski, B., Cardoso, M., Bustamante, M., Kurths, J., & Thonicke, K. (2019). Improving the LPJmL4-SPITFIRE vegetation–fire model for South America using satellite data. *Geoscientific Model Development*, 12(12), 5029–5054.

Duque, A., Muller-Landau, H. C., Valencia, R., Cardenass, D., Davies, S., de Oliveira, A., Pérez, Á. J., Romero-Saltos, H., & Vicentini, A.

(2017). Insights into regional patterns of Amazonian forest structure, diversity, and dominance from three large terra-firme forest dynamics plots. *Biodiversity and Conservation*, 26, 669–686. https://doi.org/10.1007/s10531-016-1265-9

Dybzinski, R., Farrior, C., Wolf, A., Reich, P. B., & Pacala, S. W. (2011). Evolutionary stable strategy carbon allocation to foliage, wood, and fine roots in trees competing for light and nitrogen: An analytically tractable, individual-based model and quantitative comparison to data. *The American Naturalist*, 177(2), 153–166.

E3SM Project DOE. (2018). Energy exascale earth system model.

Eyles, A., Pinkard, E. A., & Mohammed, C. (2009). Shifts in biomass and resource allocation patterns following defoliation in Eucalyptus globulus growing with varying water and nutrient supplies. *Tree Physiology*, 29(6), 753–764.

Farrior, C. E., Bohlman, S. A., Hubbell, S., & Pacala, S. W. (2016). Dominance of the suppressed: Power-law size structure in tropical forests. *Science*, 351(6269), 155–157.

Farrior, C. E., Dybzinski, R., Levin, S. A., & Pacala, S. W. (2013). Competition for water and light in closed-canopy forests: A tractable model of carbon allocation with implications for carbon sinks. *The American Naturalist*, 181(3), 314–330.

FATES Development Team. (2020). The functionally assembled terrestrial ecosystem simulator (FATES) (sci.1.35.5_api.11.0.0). *Zenodo*. https://doi.org/10.5281/zenodo.3825474

Fisher, R. A., Koven, C. D., Anderegg, W. R. L., Christoffersen, B. O., Dietze, M. C., Farrior, C. E., Holm, J. A., Hurtt, G. C., Knox, R. G., Lawrence, P. J., Lichstein, J. W., Longo, M., Matheny, A. M., Medvigy, D., Muller-Landau, H. C., Powell, T. L., Serbin, S. P., Sato, H., Shuman, J. K., … Moorcroft, P. R. (2018). Vegetation demographics in earth system models: A review of progress and priorities. *Global Change Biology*, 24(1), 35–54.

Fisher, R. A., Muszala, S., Verteinstein, M., Lawrence, P., Xu, C., McDowell, N. G., Knox, R. G., Koven, C., Holm, J., Rogers, B. M., Spessa, A., Lawrence, D., & Bonan, G. (2015). Taking off the training wheels: The properties of a dynamic vegetation model without climate envelopes, CLM4.5(ED). *Geoscientific Model Development*, 8(11), 3593–3619.

Fisher, R., McDowell, N., Purves, D., Moorcroft, P., Sitch, S., Cox, P., Huntingford, C., Meir, P., & Ian Woodward, F. (2010). Assessing uncertainties in a second-generation dynamic vegetation model caused by ecological scale limitations. *The New Phytologist*, 187(3), 666–681.

Flake, S. W., Abreu, R. C. R., Durigan, G., & Hoffmann, W. A. (2021). Savannas are not old fields: Functional trajectories of forest expansion in a fire-suppressed Brazilian savanna are driven by habitat generalists. *Functional Ecology*, 35, 1797–1809.

Friend, A. D., Lucht, W., Rademacher, T. T., Keribin, R., Betts, R., Cadule, P., Ciais, P., Clark, D. B., Dankers, R., Falloon, P. D., Ito, A., Kahana, R., Kleidon, A., Lomas, M. R., Nishina, K., Ostberg, S., Pavlick, R., Peylin, P., Schaphoff, S., … Woodward, I. (2014). Carbon residence time dominates un certainty in terrestrial vegetation responses to future climate and atmospheric CO_2. *Proceedings of the National Academy of Sciences of the United States of America*, 111(9), 3280–3285.

Gatti, L. V., Basso, L. S., Miller, J. B., Gloor, M., Gatti Domingues, L., Cassol, H. L. G., Tejada, G., Aragao, L. E. O. C., Nobre, C., Peters, W., Marani, L., Arai, E., Sanches, A. H., Correa, S. M., Anderson, L., Randow, C. V., Correia, C. S. C., Crispim, S. P., & Neves, R. A. L. (2021). Amazonia as a carbon source linked to deforestation and climate change. *Nature*, 595(7867), 388–393.

Gaylord, M. L., Kolb, T. E., Pockman, W. T., Plaut, J. A., Yepez, E. A., Macalady, A. K., Pangle, R. E., & McDowell, N. G. (2013). Drought predisposes piñon-juniper woodlands to insect attacks and mortality. *The New Phytologist*, 198(2), 567–578.

Gora, E. M., Kneale, R. C., Larjavaara, M., & Muller-Landau, H. C. (2019). Dead wood necromass in a moist tropical forest: Stocks, fluxes, and spatiotemporal variability. *Ecosystems*, 22, 1–17.

Hartmann, H., & Trumbore, S. (2016). Understanding the roles of non-structural carbohydrates in forest trees - from what we can measure to what we want to know. *The New Phytologist*, 211(2), 386–403.

Henkel, T. K., Chambers, J. Q., & Baker, D. A. (2016). Delayed tree mortality and Chinese tallow (*Triadica sebifera*) population explosion in a Louisiana bottomland hardwood forest following hurricane Katrina. *Forest Ecology and Management*, 378, 222–232.

Herguido, E., Granda, E., Benavides, R., García-Cervigón, A. I., Camarero, J. J., & Valladares, F. (2016). Contrasting growth and mortality responses to climate warming of two pine species in a continental Mediterranean ecosystem. *Forest Ecology and Management*, 363, 149–158.

Hogan, J., Zimmerman, J., Thompson, J., Uriarte, M., Swenson, N., Condit, R., Hubbell, S., Johnson, D. J., Sun, I. F., Chang-Yang, C.-H., Su, S.-H., Ong, P., Rodriguez, L., Monoy, C. C., Yap, S., & Davies, S. J. (2018). The frequency of cyclonic wind storms shapes tropical forest dynamism and functional trait dispersion. *Forests*, 9(7), 404.

Hurtt, G. C., Chini, L., Sahajpal, R., Frolking, S., Bodirsky, B. L., Calvin, K., Doelman, J. C., Fisk, J., Fujimori, S., Klein Goldewijk, K., Hasegawa, T., Havlik, P., Heinimann, A., Humpenöder, F., Jungclaus, J., Kaplan, J. O., Kennedy, J., Krisztin, T., Lawrence, D., ... Zhang, X. (2020). Harmonization of global land use change and management for the period 850–2100 (LUH2) for CMIP6. *Geoscientific Model Development*, 13(11), 5425–5464.

Jönsson, A. M., Schroeder, L. M., Lagergren, F., Anderbrant, O., & Smith, B. (2012). Guess the impact of Ips typographus—An ecosystem modelling approach for simulating spruce bark beetle outbreaks. *Agricultural and Forest Meteorology*, 166–167, 188–200.

Koven, C. D., Chambers, J. Q., Georgiou, K., Knox, R., Negron-Juarez, R., Riley, W. J., Arora, V. K., Brovkin, V., Friedlingstein, P., & Jones, C. D. (2015). Controls on terrestrial carbon feedbacks by productivity versus turnover in the CMIP5 earth system models. *Biogeosciences*, 12(17), 5211–5228.

Koven, C. D., Knox, R. G., Fisher, R. A., Chambers, J. Q., Christoffersen, B. O., Davies, S. J., Detto, M., Dietze, M. C., Faybishenko, B., Holm, J., Huang, M., Kovenoch, M., Kueppers, L. M., Lemieux, G., Massoud, E., McDowell, N. G., Muller-Landau, H. C., Needham, J. F., Norby, R. J., ... Xu, C. (2020). Benchmarking and parameter sensitivity of physiological and vegetation dynamics using the functionally assembled terrestrial ecosystem simulator (FATES) at Barro Colorado Island. *Panama. Biogeosciences*, 17(11), 3017–3044.

Lagergren, F., Jönsson, A. M., Blennow, K., & Smith, B. (2012). Implementing storm damage in a dynamic vegetation model for regional applications in Sweden. *Ecological Modelling*, 247, 71–82.

Lawrence, D. M., Fisher, R. A., Koven, C. D., Oleson, K. W., Swenson, S. C., Bonan, G., Collier, N., Ghimire, B., van Kampenhout, L., Kennedy, D., Kluzek, E., Lawrence, P. J., Li, F., Li, H., Lombardozzi, D., Riley, W. J., Sacks, W. J., Shi, M., Vertenstein, M., Wieder, W. R., ... Zeng, X. (2019). The community land model version 5: Description of new features, benchmarking, and impact of forcing uncertainty. *Journal of Advances in Modeling Earth Systems*, 11, 4245–4287.

Liu, X., Zeng, X., Zou, X., González, G., Wang, C., & Yang, S. (2018). Litterfall production prior to and during hurricanes Irma and Maria in four Puerto Rican forests. *Forests*, 9(6), 367.

Lodge, D. J., Scatena, F. N., Asbury, C. E., & Sanchez, M. J. (1991). Fine litterfall and related nutrient inputs resulting from hurricane Hugo in subtropical wet and lower montane rain forests of Puerto Rico. *Biotropica*, 23(4), 336.

Malhi, Y., Farfán Amézquita, F., Doughty, C. E., Silva-Espejo, J. E., Girardin, C. A. J., Metcalfe, D. B., Aragao, L. E. O. C., Huaraca-Quispe, L. P., Alzamora-Taype, I., Eguiluz-Mora, L., Marthews, T. R., Halladay, K., Quesada, C. A., Robertson, A. L., Fisher, J. B., Zaragoza-Castells, J., Rojas-Villagra, C. M., Pelaez-Tapia, Y., ... Phillips, O. L. (2014). The productivity, metabolism and carbon cycle of two lowland tropical forest plots in South-Western Amazonia. *Peru. Plant Ecology and Diversity*, 7(1–2), 85–105.

Malhi, Y., Girardin, C. A. J., Goldsmith, G. R., Doughty, C. E., Salinas, N., Metcalfe, D. B., Huaraca Huasco, W., Silva-Espejo, J. E., Aguilla-Pasquell, J., Farfán Amézquita, F., Aragão, L. E. O. C., Guerrieri, R., Ishida, F. Y., Bahar, N. H. A., Farfan-Rios, W., Phillips, O. L., Meir, P., & Silman, M. (2017). The variation of productivity and its allocation along a tropical elevation gradient: A whole carbon budget perspective. *The New Phytologist*, 214(3), 1019–1032.

Martínez Cano, I., Shevliakova, E., Malyshev, S., Wright, S. J., Detto, M., Pacala, S. W., & Muller-Landau, H. C. (2020). Allometric constraints and competition enable the simulation of size structure and carbon fluxes in a dynamic vegetation model of tropical forests (LM3PPA-TV). *Global Change Biology*, 26(8), 4478–4494.

Marvin, D. C., & Asner, G. P. (2016). Branchfall dominates annual carbon flux across lowland Amazonian forests. *Environmental Research Letters*, 11(9), 094027.

McDowell, N. G., & Sevanto, S. (2010). The mechanisms of carbon starvation: How, when, or does it even occur at all? *The New Phytologist*, 186(2), 264–266.

McDowell, N., Allen, C. D., Anderson-Teixeira, K., Brando, P., Brienen, R., Chambers, J., Christoffersen, B., Davies, S., Doughty, C., Duque, A., Espirito-Santo, F., Fisher, R., Fontes, C. G., Galbraith, D., Goodsman, D., Grossiord, C., Hartmann, H., Holm, J., Johnson, D. J., ... Xu, X. (2018). Drivers and mechanisms of tree mortality in moist tropical forests. *The New Phytologist*, 219(3), 851–869.

McDowell, N., Pockman, W. T., Allen, C. D., Breshears, D. D., Cobb, N., Kolb, T., Plaut, J., Sperry, J., West, A., Williams, D. G., & Yepez, E. A. (2008). Mechanisms of plant survival and mortality during drought: Why do some plants survive while others succumb to drought? *The New Phytologist*, 178(4), 719–739.

Moorcroft, P. R., Hurtt, G. C., & Pacala, S. W. (2001). A method for scaling vegetation dynamics: The ecosystem demography model (ed). *Ecological Monographs*, 71(4), 557–586.

Needham J., Arellano G., Davies S., Fisher R., Hammer V., Knox R., Mitre D., Muller-Landau H., Zuleta D., Koven C. (2022): FATES crown damage simulation outputs 2022. 1.0. NGEE Tropics Data Collection. (dataset). https://doi.org/10.15486/ngt/1871026

Negrón-Juárez, R. I., Holm, J. A., Faybishenko, B., Magnabosco-Marra, D., Fisher, R. A., Shuman, J. K., de Araujo, A. C., Riley, W. J., & Chambers, J. Q. (2020). Landsat near-infrared (NIR) band and ELM-FATES sensitivity to forest disturbances and regrowth in the Central Amazon. *Biogeosciences*, 17(23), 6185–6205.

Newbery, D. M., & Zahnd, C. (2021). Change in liana density over 30 years in a Bornean rain forest supports the escape hypothesis. *Ecosphere*, 12(8), e03537. https://doi.org/10.1002/ecs2.3537

Oleson, K., Lawrence, D., Bonan, G., Drewniak, B., Huang, M., Koven, C. D., Levis, S., Li, F., Riley, W. J., Subin, Z. M., Swenson, S., Thornton, P. E., Bozbiyik, A., Risher, R., Heald, C. L., Kluzek, E., Lamarque, J.-F., Lawrence, P. J., Leung, R. L., ... Yang, Z.-L. (2013). Technical description of version 4.5 of the community land model (CLM). *UCAR/NCAR*.

Pachzelt, A., Forrest, M., Rammig, A., Higgins, S. I., & Hickler, T. (2015). Potential impact of large ungulate grazers on African vegetation, carbon storage and fire regimes. *Global Ecology and Biogeography*, 24(9), 991–1002.

Paz, H., Vega-Ramos, F., & Arreola-Villa, F. (2018). Understanding hurricane resistance and resilience in tropical dry forest trees: A functional traits approach. *Forest Ecology and Management*, 426, 115–122.

Peñuelas, J., Ciais, P., Canadell, J. G., Janssens, I. A., Fernández-Martínez, M., Carnicer, J., Obersteiner, M., Piao, S., Vautard, R., & Sardans, J. (2017). Shifting from a fertilization-dominated to a warming-dominated period. *Nature Ecology and Evolution*, 1(10), 1438–1445.

Poorter, L., Bongers, F., Sterck, F. J., & Woll, H. (2005). Beyond the regeneration phase: Differentiation of height-light trajectories among tropical tree species. *Journal of Ecology*, 93(2), 256–267.

Powell, T. L., Koven, C. D., Johnson, D. J., Faybishenko, B., Fisher, R. A., Knox, R. G., McDowell, N. G., Condit, R., Hubbell, S. P., Wright, S. J., Chambers, J. Q., & Kueppers, L. M. (2018). Variation in hydroclimate sustains tropical forest biomass and promotes functional diversity. *The New Phytologist*, 219(3), 932–946.

Purves, D. W., Lichstein, J. W., Strigul, N., & Pacala, S. W. (2008). Predicting and understanding forest dynamics using a simple tractable model. *Proceedings of the National Academy of Sciences of the United States of America*, 105(44), 17018–17022.

Ramos, P., Villareal, P., Condit, R., Cushman, K., & Muller-Landau, H. (2022). Annual dendrometer data from the Barro Colorado Island 50-ha forest dynamics plot for 2015-2020. *Smithsonian Figshare*. https://doi.org/10.25573/data.19985066

Reis, S. M., Marimon, B. S., Esquivel-Muelbert, A., Marimon, B. H., Morandi, P. S., Elias, F., de Oliveira, E. A., Galbraith, D., Feldpausch, T. R., Menor, I. O., Malhi, Y., & Phillips, O. I. L. (2022). Climate and crown damage drive tree mortality in southern Amazonian edge forests. *Journal of Ecology*, 110, 876–888.

Reis, S. M., Marimon, B. S., Morandi, P. S., Elias, F., Esquivel-Muelbert, A., Marimon Junior, B. H., Fauset, S., Oliveira, E. A., Heijden, G. M. F., Galbraith, D., Feldpausch, T. R., & Phillips, O. L. (2020). Causes and consequences of liana infestation in southern Amazonia. *Journal of Ecology*, 108(6), 2184–2197.

Rood, S. B., Patiño, S., Coombs, K., & Tyree, M. T. (2000). Branch sacrifice: Cavitation-associated drought adaptation of riparian cottonwoods. *Trees*, 14(5), 0248–0257.

Rowland, L., da Costa, A. C. L., Galbraith, D. R., Oliveira, R. S., Binks, O. J., Oliveira, A. A. R., Pullen, A. M., Doughty, C. E., Metcalfe, D. B., Vasconcelos, S. S., Ferreira, L. V., Malhi, Y., Grace, J., Mencuccini, M., & Meir, P. (2015). Death from drought in tropical forests is triggered by hydraulics not carbon starvation. *Nature*, 528(7580), 119–122.

Sala, A., Woodruff, D. R., & Meinzer, F. C. (2012). Carbon dynamics in trees: Feast or famine? *Tree Physiology*, 32(6), 764–775.

Seidl R., Klonner G., Rammer W., Essl F., Moreno A., Neumann M., Dullinger S. 2018. Invasive alien pests threaten the carbon stored in Europe's forests. *Nature Communications* 9(1):1626, 9

Senf, C., Pflugmacher, D., Zhiqiang, Y., Sebald, J., Knorn, J., Neumann, M., Hostert, P., & Seidl, R. (2018). Canopy mortality has doubled in Europe's temperate forests over the last three decades. *Nature Communications*, 9(1), 4978.

Stevens, M. T., Kruger, E. L., & Lindroth, R. L. (2008). Variation in tolerance to herbivory is mediated by differences in biomass allocation in Aspen. *Functional Ecology*, 22, 40–47.

Tanner, E. V. J., Rodriguez-Sanchez, F., Healey, J. R., Holdaway, R. J., & Bellingham, P. J. (2014). Long-term hurricane damage effects on tropical forest tree growth and mortality. *Ecology*, 95(10), 2974–2983.

Taylor, S. L., & MacLean, D. A. (2009). Legacy of insect defoliators: Increased wind-related mortality two decades after a spruce budworm outbreak. *Forest Science*, 55(3), 256–267.

Trenberth, K. E., Dai, A., van der Schrier, G., Jones, P. D., Barichivich, J., Briffa, K. R., & Sheffield, J. (2013). Global warming and changes in drought. *Nature Climate Change*, 4(1), 17–22.

Trugman, A. T., Detto, M., Bartlett, M. K., Medvigy, D., Anderegg, W. R. L., Schwalm, C., Schaffer, B., & Pacala, S. W. (2018). Tree carbon allocation explains forest drought-kill and recovery patterns. *Ecology Letters*, 21(10), 1552–1560.

Umaña, M. N., & Arellano, G. (2021). Legacy effects of drought on tree growth responses to hurricanes. *Ecography*, 44, 1686–1697. https://doi.org/10.1111/ecog.05803

Uriarte, M., Canham, C. D., Thompson, J., & Zimmerman, J. K. (2004). A neighborhood analysis of tree growth and survival in a hurricane-driven tropical forest. *Ecological Monographs*, 74(4), 591–614.

Ver Planck, N. R., & MacFarlane, D. W. (2014). Modelling vertical allocation of tree stem and branch volume for hardwoods. *Forestry*, 87(3), 459–469.

Westerling, A. L., Turner, M. G., Smithwick, E. A. H., Romme, W. H., & Ryan, M. G. (2011). Continued warming could transform greater Yellowstone fire regimes by mid-21st century. *Proceedings of the National Academy of Sciences of the United States of America*, 108(32), 13165–13170.

Yang, Y., Saatchi, S. S., Xu, L., Yu, Y., Choi, S., Phillips, N., Kennedy, R., Keller, M., Knyazikhin, Y., & Myneni, R. B. (2018). Post-drought decline of the Amazon carbon sink. *Nature Communications*, 9(1), 3172.

Zuleta, D., Arellano, G., Muller-Landau, H. C., McMahon, S. M., Aguilar, S., Bunyavejchewin, S., Cardenas, D., Chang-Yang, C.-H., Duque, A., Mitre, D., Sasardin, M., Perez, R., Sun, I.-F., Yao, T. L., & Davies, S. J. (2021). Individual tree damage dominates mortality risk factors across six tropical forests. *The New Phytologist*, 233, 705–721.

Zuleta, D., Krishna Moorthy, S. M., Arellano, G., Verbeeck, H., & Davies, S. J. (2022). Vertical distribution of trunk and crown volume in tropical trees. *Forest Ecology and Management*, 508, 120056.

SUPPORTING INFORMATION

Additional supporting information can be found online in the Supporting Information section at the end of this article.